Frequency measurement of the $^2\mathbf{S}_{1/2} - {}^2\mathbf{D}_{3/2}$ electric quadrupole transition in a single $^{171}\mathrm{Yb}^+$ ion

Stephen Webster, Rachel Godun, Steven King, Guilong Huang, Barney Walton
Veronika Tsatourian, Helen Margolis, Stephen Lea and Patrick Gill
National Physical Laboratory, Hampton Road, Middlesex, TW11 0LW, UK
Email: stephen.webster@npl.co.uk

***Abstract*— We report on precision laser spectroscopy of the $^2\mathbf{S}_{1/2}(F=0) - {}^2\mathbf{D}_{3/2}(F=2, m_F=0)$ clock transition in a single ion of $^{171}\mathrm{Yb}^+$. The absolute value of the transition frequency, determined using an optical frequency comb referenced to a hydrogen maser, is 688 358 979 309 310 ± 9 Hz. This corresponds to a fractional uncertainty of 1.3×10^{-14}.**

I. Introduction

Optical frequency standards now offer unprecedented precision, with uncertainties at the part in 10^{16} level and below having been reported [1], [2]. Experimental resolution at this level opens up the possibility for making precise tests of fundamental physics. In particular, a direct comparison of two optical frequencies places a limit on the time variation of the fine-structure constant ($\dot{\alpha}$) [3] and following the comparison between optical transitions in Hg^+ and Al^+, this limit now stands at $\partial \ln \alpha / \partial t = (-1.6 \pm 2.3) \times 10^{-17}$ year^{-1} [2].

Theoretical predictions for the sensitivity of the transitions in Yb^+ to $\dot{\alpha}$ mark it out as being of particular interest [3]. The partial term scheme is shown in Fig. 1. The $^2\mathrm{F}_{7/2}$ state has the largest known sensitivity to $\dot{\alpha}$ and its dependence is of the opposite sign to that of the $^2\mathrm{D}_{3/2}$ state. A measurement of the ratio of the $^2\mathrm{S}_{1/2} - {}^2\mathrm{D}_{3/2}$, electric quadrupole (E2) transition at 688 THz (436 nm) and the $^2\mathrm{S}_{1/2} - {}^2\mathrm{F}_{7/2}$, electric octupole (E3) transition at 642 THz (467 nm) yields a sensitivity to $\dot{\alpha}$ of [4], [5]

$$\frac{\partial}{\partial t} \ln \frac{f_{\mathrm{Yb}^+(\mathrm{E2})}}{f_{\mathrm{Yb}^+(\mathrm{E3})}} = 6.8 \frac{\partial}{\partial t} \ln \alpha. \qquad (1)$$

Further, the ratio measurement may be conducted in the same ion and this gives rise to significant common mode-rejection of systematic frequency shifts. There will be no dependence on those shifts associated with the motion of the ion and the fact that the ion experiences an identical field irrespective of the transition being measured will lead to more accurate determinations of the field-dependent shifts. To put a limit on variation of α with an uncertainty $< 1 \times 10^{-17}$ year^{-1}, on a one-year timescale, will require that the ratio be measured with an uncertainty of $< 5 \times 10^{-17}$.

Both the E2 and E3 transitions are currently being developed as optical frequency standards. The frequency of the E2 transition has been measured with an uncertainty of 3×10^{-15} and two frequency standards operating on the E2 transition have been compared with a relative uncertainty of 4×10^{-16} [6].

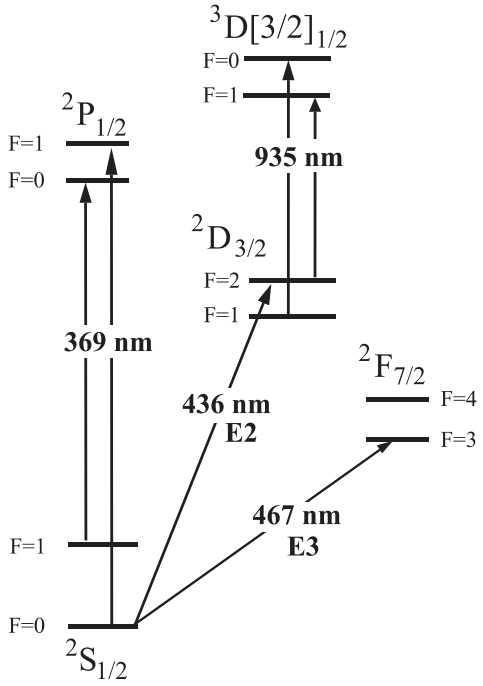

Fig. 1. Partial term scheme for $^{171}\mathrm{Yb}^+$, showing the cooling transition at 369 nm and the E2 and E3 electric quadrupole and electric octupole transitions at 436 nm and 467 nm respectively. The metastable $^2\mathrm{D}_{3/2}$ state is depopulated by laser radiation at 935 nm.

The frequency of the E3 transition has been measured with an uncertainty of 2×10^{-14} [7]. Here we report the development of a laser source at 436 nm and an independent measurement of the E2 transition with an uncertainty of 1.3×10^{-14}.

II. Experimental Setup

The experimental scheme is shown in Fig. 2. A single ion is confined in an endcap trap and is Doppler cooled on the $^2\mathrm{S}_{1/2}(F=1) - {}^2\mathrm{P}_{1/2}(F=0)$ transition at 369 nm. The ion can decay to the $^2\mathrm{D}_{3/2}(F=1)$ level, so light at 935 nm is used to drive the $^2\mathrm{D}_{3/2}(F=1) - {}^3\mathrm{D}[3/2]_{1/2}(F=0)$ transition and return the ion to the $F=1$ ground state. Spontaneous Raman transitions can occur to the $^2\mathrm{S}_{1/2}(F=0)$ and $^2\mathrm{D}_{3/2}(F=2)$ levels via the $^2\mathrm{P}_{1/2}(F=1)$ level, and so two further frequencies are required to maintain continuous cooling. Sidebands at 14.75 GHz are applied to the light at 369 nm using a resonant

978-1-4244-3510-4/09/$25.00 ©2009 Crown

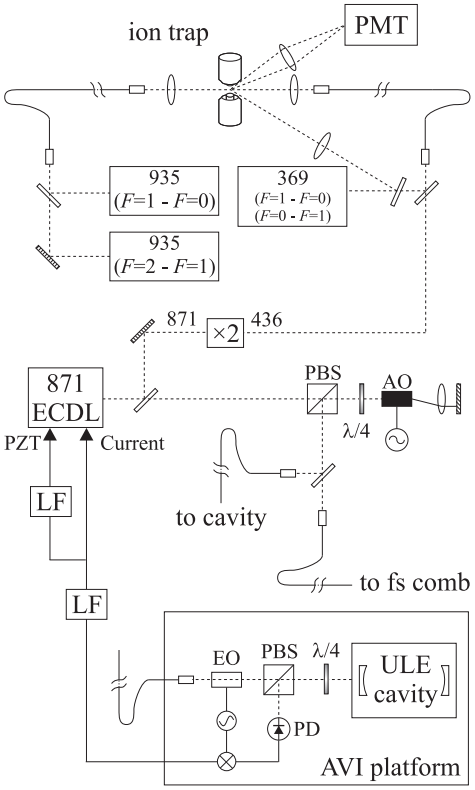

Fig. 2. Schematic showing the probe laser system and beam delivery to the ion trap. AO: acousto-optic modulator; EO: electro-optic modulator; $\lambda/4$: quarter-wave plate; PBS: polarizing beam-splitter; PD: avalanche photodiode; PMT: photomultiplier tube; LF: loop filter; AVI: active vibration isolation; ECDL: extended cavity diode laser; PZT: piezoelectric transducer; ULE: ultra-low expansivity. The laser systems are represented by boxes showing their wavelength in nm. The dashed lines indicate laser beam paths and the solid lines indicate optical fibres or electrical signal paths.

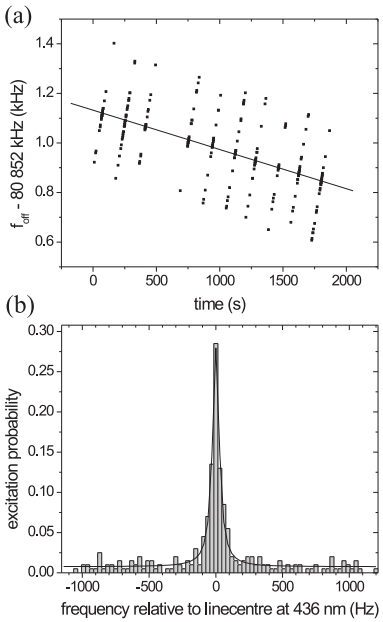

Fig. 3. (a) Plot showing the offset frequency, $f_{\rm off}$, as described in equation 2, corresponding to individual quantum jumps as a function of time for 10 scans of the probe laser frequency across the 436 nm transition. A linear fit to the data yields a slope of -0.16 Hz/s, corresponding to a cavity drift rate of -0.32 Hz/s. (b) Atomic absorption spectrum of the $^2\mathrm{S}_{1/2}(F=0) - {}^2\mathrm{D}_{3/2}(F=2)$ transition at 436 nm. The bin width is 20 Hz and a Lorentzian fit to the data has a full-width at half-maximum (FWHM) of 61 Hz.

cavity electro-optic modulator operating at 7.375 GHz to drive the $^2\mathrm{S}_{1/2}(F=0) - {}^2\mathrm{P}_{1/2}(F=1)$ transition. A second laser at 935 nm is used to drive the $^2\mathrm{D}_{3/2}(F=2) - {}^3\,\mathrm{D}[3/2]_{1/2}(F=1)$ transition. The ion is prepared in the $^2\mathrm{S}_{1/2}(F=0)$ ground state by removing the sidebands on the 369 nm light, following which it is probed on the $^2\mathrm{S}_{1/2}(F=0) - {}^2\mathrm{D}_{3/2}(F=2)$ transition with light at 436 nm. Fluorescence from the cooling transition is observed with a photomultiplier tube and quantum jumps to the $^2\mathrm{D}_{3/2}(F=2)$ state are detected through the absence of this fluorescence.

During detection, it is important not to depopulate the upper, $^2\mathrm{D}_{3/2}(F=2)$, state, otherwise a false negative is recorded. Therefore, the 935 nm $F=2-F=1$ beam is switched off during this period. The laser tuned to the 935 nm $F=1-F=0$ transition can off-resonantly drive the ion out of the $^2\mathrm{D}_{3/2}(F=2)$ state. To prevent this, the intensity is reduced and the light is filtered by a Fabry-Pérot etalon to remove the spontaneous emission from the diode. Spontaneous Raman transitions to the $^2\mathrm{D}_{3/2}(F=2)$ state via the $^2\mathrm{P}_{1/2}(F=1)$ level still occur during detection, being observed as quantum jumps in the fluorescence, and this leads to an unavoidable background of false positives. To check that the intensity of the 935 nm $\mathrm{F}=1-\mathrm{F}=0$ light has been sufficiently reduced, a measurement is made of the average duration of the quantum jumps in the fluorescence. In the limit of there being no light at 935 nm, the $^2\mathrm{D}_{3/2}$ state lifetime is 50 ms; with a strong beam at 935 nm, no quantum jumps are seen in the fluorescence. By reducing the 935 nm intensity to below saturation on the transition, the lifetime can be extended to 40 ms without significant reduction in the signal-to-noise of the detected fluorescence; however, some level of depopulation of the $^2\mathrm{D}_{3/2}(F=2)$ state is still unavoidable during detection.

Light at 435.5 nm is generated by frequency doubling a diode laser at 871.0 nm. The second harmonic is generated in a single pass through a crystal of $KNbO_3$ configured for non-critical phase-matching at 57°C. Up to 12μW of power at 436 nm is generated for an input power of 30 mW. The diode laser is set up in a temperature-controlled, monolithic extended cavity in the Littrow configuration. The reflectivity of the output facet of the diode, R, is less than 5×10^{-5}; thus, the frequency of operation is largely governed by the 8 % feedback from the grating of the extended cavity and up to 50 mW is generated in a single mode. The frequency of the diode laser is locked to a mode of a 10 cm-long optical cavity with a finesse of 100,000 using the Pound-Drever-Hall technique. Fast feedback is to the diode current and slow feedback is to a piezoelectric transducer controlling the extended cavity length. The loop filter is a single op-amp with proportional, integral and differential gain and is set up to compensate

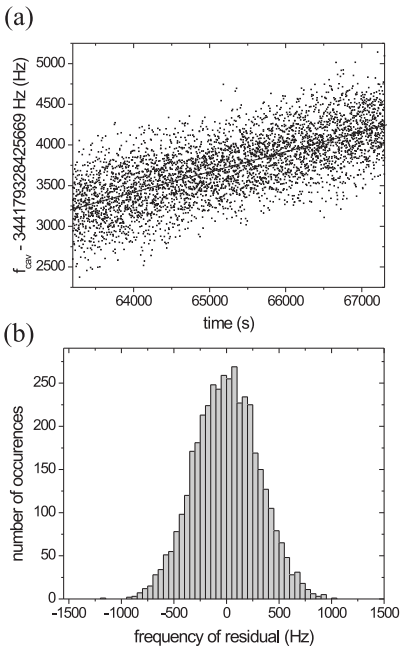

Fig. 4. (a) Sample data showing the frequency of the ULE cavity mode measured by the optical frequency comb. Each point is a 1 s average. The solid line is a third-order polynomial fit to the data. (b) Histogram showing the residuals of the fit. The standard deviation and standard error of the mean are 306 Hz and 4.8 Hz respectively.

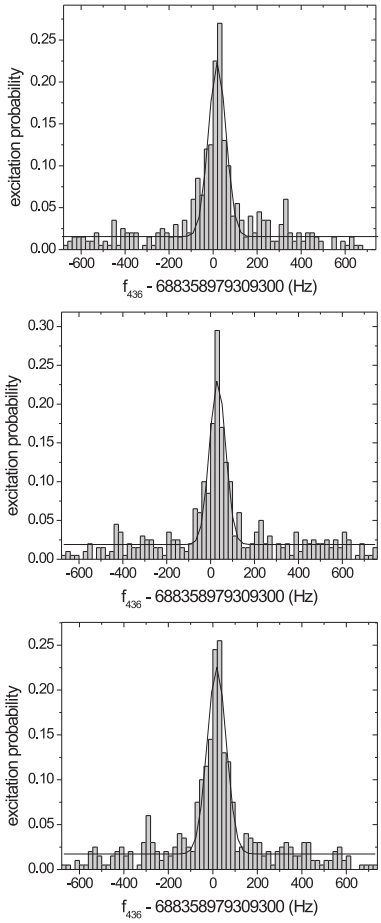

Fig. 5. Absorption spectrum as a function of frequency for three orthogonal magnetic fields with $|B| = 6\,\mu$T. The solid lines are Gaussian fits to the data. Starting from the upper figure and descending, the mean centre frequencies are 18.7 ± 2.5, 31.7 ± 2.4, and 17.3 ± 2.3 Hz respectively. These values do not include corrections for the second-order Zeeman shift, the Blackbody Stark shift or the deviation of the maser reference frequency from 10 MHz.

for the integral response introduced by the cavity at 15 kHz and the phase-lag of the diode's response which reaches 90° at 500 kHz. A servo bandwidth of > 100 kHz is achieved which is sufficient to reduce the in-loop frequency noise at Fourier-frequencies in the range 1–100 Hz to an amplitude < 1 Hz. The cavity, made from ultra-low-expansivity glass, is temperature controlled at 3°C, where it has zero linear expansion, and is mounted within a vacuum chamber situated on an active vibration isolation platform. The cavity spacer is of a cylindrical geometry, modified with square cut-outs, to reduce its sensitivity to vibrations [8].

The frequency of the light at 436 nm is given by

$$f_{436} = 2(f_{\mathrm{cav}} + 2f_{\mathrm{off}}), \tag{2}$$

where f_{cav} is the frequency of the cavity mode and f_{off} is a frequency offset provided by a double-passed acousto-optic modulator (AOM). The frequency of the 436 nm light is tuned by stepping this offset, whilst maintaining the lock to the cavity. To observe the atomic transition, the laser is repeatedly scanned over the transition and the offset frequency corresponding to individual quantum jumps is recorded. The data are shown in Fig. 3(a). The cavity drift is removed and the data are collated to give the atomic absorption spectrum shown in Fig. 3(b). The probe beam has a power of 1 nW, focused to a spot with a diameter $\sim 100\,\mu$m and is pulsed on for a duration of 30 ms and. Under these conditions, the transition is well below saturation. A Lorentzian fit to the data has a width (FWHM) of 61 Hz. This is largely attributed to the width of the probe laser at a timescale of 30 minutes, the period over which the measurement is performed.

III. Absolute frequency measurement

To measure the absolute frequency of the transition, the frequency of the light locked to the cavity is measured using an optical frequency comb based on a mode-locked erbium-doped fibre laser [9], whilst simultaneously scanning the probe laser over the transition. The synthesizer generating the offset frequency and those used in the optical frequency comb are referenced to the 10 MHz output of a hydrogen maser which forms part of the clock ensemble used to generate the NPL(UTC) time scale. Fig. 4(a) shows a sample set of data for the frequency comb measurement. The data-acquisition systems for the ion trap and the optical frequency comb are synchronized and the fit to the frequency comb data is used to calculate the frequency at 436 nm of each quantum jump using (2). The measurement is repeated over a range of magnetic

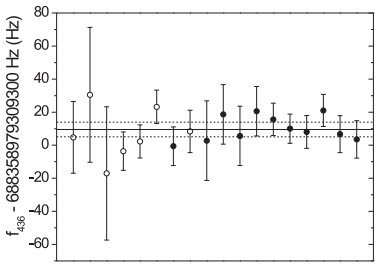

Fig. 6. Frequency of the $^2\mathrm{S}_{1/2}(F=0) - {}^2\mathrm{D}_{3/2}(F=2, m_F=0)$ clock transition in $^{171}\mathrm{Yb}^+$. The data are taken over a range of magnetic field amplitudes and directions. Corrections for the deviation of the maser reference frequency from 10 MHz, as determined by comparison with UTC, the second-order Zeeman shift and the Blackbody Stark shift are included. The solid line is a weighted mean of all the data and the dashed lines indicate a 1σ uncertainty. The data taken over three orthogonal directions of the magnetic field are shown as filled circles.

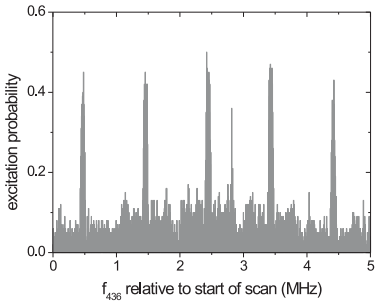

Fig. 7. Probe laser scan over 5 MHz showing frequency carrier and radial and axial sidebands. The radial and axial frequencies, derived from the sideband separations, are $\omega_r = 2\pi \times 0.9865\,\mathrm{MHz}$ and $\omega_z = 2\pi \times 1.975\,\mathrm{MHz}$ respectively. The feature at 2.8 MHz is spurious.

field amplitudes and orientations to test for the presence of a quadrupole shift and, for a subset of these measurements, the field directions form an orthogonal basis set. The shift is given by [10]

$$\Delta\nu = \frac{Q_{\mathrm{dc}}\Theta(\mathrm{D}_{3/2})}{h}(3\cos^2\theta - 1), \tag{3}$$

where Q_{dc} is a dc quadrupole field and θ is the angle between the magnetic and quadrupole fields, and averages to zero over three orthogonal directions of the magnetic field [11]. Fig. 5 shows a sample set of data for each of three orthogonal field directions. The complete set of measurements is shown in Fig. 6. Each point is corrected for the second-order Zeeman shift, the deviation of the maser reference frequency from 10 MHz as determined by comparison with UTC and a Blackbody Stark shift of -0.36 Hz [12]. The error bars include contributions from the error on the mean of the transition frequency data, the standard error on the mean of the fit to the frequency comb data and the error on the correction for the Zeeman shift. There is no significant correlation between the frequency and magnetic field direction; therefore, the quadrupole shift is unresolved at this level of precision. The weighted mean of the all the data is $688\ 358\ 979\ 309\ 309.9 \pm 4.4$ Hz. Analyzing the data taken over three orthogonal directions of the magnetic field, the weighted means for the three directions, in the last three significant figures, are 6.4 ± 15.8, 18.4 ± 20.8 and 8.3 ± 21.0 Hz. An unweighted mean of these values gives $688\ 358\ 979\ 309\ 311.1 \pm 11.1$ Hz which is consistent with there being no significant bias to the weighted mean of the complete set of data.

As an independent check, the quadrupole shift is derived from a measurement of the secular frequencies of the ion's motion in the trap. Fig. 7 shows the absorbtion spectrum taken over a frequency range of 5 MHz and includes the first radial and axial secular sidebands. The secular frequencies are given by $\omega_i = \beta_i\Omega/2$, where $i \in r, z$, Ω is the trap drive frequency and β is given to fourth order in q_i by [13]

$$\beta_i^2 = a_i - \left(\frac{a_i - 1}{2(a_i-1)^2 - q_i^2}\right) q_i^2 - \left(\frac{5a_i + 7}{32(a_i-1)^3(a_i-4)}\right) q_i^4. \tag{4}$$

For the trap potential, $\phi = (Q_{\mathrm{dc}} + Q_{\mathrm{ac}}\cos\Omega t)(r^2 - 2z^2)$, where Q_{dc} and Q_{ac} are the dc and ac quadrupole fields respectively, the parameters, a_i and q_i are defined as

$$a_r = -\frac{a_z}{2} = +\frac{8eQ_{\mathrm{dc}}}{m\Omega^2} \tag{5}$$

$$q_r = -\frac{q_z}{2} = -\frac{4eQ_{\mathrm{ac}}}{m\Omega^2} \tag{6}$$

With $\Omega = 12.8\,\mathrm{MHz}$, $\omega_r = 2\pi \times 0.9865\,\mathrm{MHz}$ and $\omega_z = 2\pi \times 1.975\,\mathrm{MHz}$, a numerical solution of (4) gives for the dc quadrupole field, $Q_{\mathrm{dc}} = 129\,\mathrm{V/cm^2}$. The quadrupole moment of the $^2\mathrm{D}_{3/2}$ state, $\Theta(\mathrm{D}_{3/2}) = 9.32 \times 10^{-40}\,\mathrm{Cm}^2$ [12] and, using (3), this gives a maximum quadrupole shift from zero of 3.6 Hz. The magnitude of quadrupole shift is again consistent with there being no significant bias in the weighted mean of all the data compared to the mean over three orthogonal field directions. However, as a conservative estimate of the uncertainty, the maximum shift is added in quadrature to the error on the weighted mean of all the data. A systematic uncertainty in the correction for the maser reference frequency of 1×10^{-14} or 6.9 Hz and the uncertainty in the Blackbody Stark shift of 0.07 Hz are also added in quadrature to the error on the weighted mean. Other systematic shifts, such as the second-order Doppler shift and the ac and dc Stark shifts, do not contribute significantly at this level. This gives, for the frequency of the $^2\mathrm{S}_{1/2}(F=0) - {}^2\mathrm{D}_{3/2}(F=2, m_F=0)$ transition, a value of $688\ 358\ 979\ 309\ 309.9 \pm 8.9$ Hz.

IV. Summary and Outlook

An experiment is described in which a single laser-cooled, trapped ion of $^{171}\mathrm{Yb}^+$ is probed on the $^2\mathrm{S}_{1/2}(F=0) - {}^2\mathrm{D}_{3/2}(F=2)$ electric quadrupole transition with light at 436 nm. In detecting quantum jumps due to absorption of the probe laser light, care is taken to minimize false events due

to off-resonant excitation, which are inherent to the detection scheme, whilst maintaining an adequate signal-to-noise level. Light at 436 nm is generated by frequency doubling a diode laser and this is actively stabilised to a temperature- and vibration-insensitive optical cavity. The atomic absorption spectrum is observed to have a width (FWHM) of 61 Hz. An absolute frequency measurement is made by simultaneously measuring the frequency of the probe laser using a femtosecond laser frequency comb referenced to a hydrogen maser. Measurements are made with different magnetic field directions to test for the presence of a quadrupole shift, but the shift is not resolved at this level of precision. An independent measurement using the trap secular frequencies puts the maximum value of the shift at 3.6 Hz and this is used as a conservative estimate of the uncertainty. The absolute frequency of the $^2\mathrm{S}_{1/2}(F=0) - {}^2\mathrm{D}_{3/2}(F=2, m_F=0)$ is determined to be $688\ 358\ 979\ 309\ 310 \pm 9$ Hz, corresponding to a fractional frequency uncertainty of 1.3×10^{-14}. The value is in good agreement with the previous reported value of $688\ 358\ 979\ 309\ 307.6 \pm 2.2$ Hz [6].

The absolute frequencies of the E2 and E3 transitions in $^{171}\mathrm{Yb}^+$ have both been measured to the part in 10^{14} level using the same apparatus. This opens up the prospect of a simultaneous ratio measurement in the same ion with the aim of putting a strict limit on the time variation of the fine-structure constant (see also [14]). The statistical uncertainty of the measurement is currently limited by the stability of the hydrogen maser and the method of data acquisition where the probe laser is repeatedly scanned over the transition. Direct comparison of the optical frequencies via the frequency comb [15] will remove the need for referencing to a hydrogen maser and stabilization of the probe laser to the atomic transition will greatly improve the data rate and reduce the statistical uncertainty. A detailed analysis of the systematic uncertainties associated with the two transitions is presented in Ref. [3]. Particular attention will need to be made to the control of the magnetic field and measurement of the ambient temperature in the trap and, for an evaluation of the ratio at the part in 10^{17} level, their respective uncertainties will need to be reduced to the 50 nT and 1 K level.

ACKNOWLEDGMENT

The authors would like to thank Geoffrey Barwood for assistance with the numerical solution of (4). This work was supported by the UK National Measurement System Pathfinder Metrology Program.

REFERENCES

[1] A. D. Ludlow, T. Zelevinsky, G. K. Campbell, S. Blatt, M. M. Boyd, M. H. G. de Miranda, M. J. Martin, J. W. Thomsen, S. M. Foreman, J. Ye, T. M. Fortier, J. E. Stalnaker, S. A. Diddams, Y. L. Coq, Z. W. Barber, N. Poli, N. D. Lemke, and C. W. Oates, "Sr lattice clock at 1×10^{-16} fractional uncertainty be remote optical evaluation with a ca clock," *Science*, vol. 319, p. 1805, 2008.

[2] T. Rosenband, D. B. Hume, P. O. Schmidt, C. W. Chou, A. Brusch, L. Lorini, W. H. Oskay, R. E. Drullinger, T. M. Fortier, J. E. Stalnaker, S. A. Diddams, W. C. Swann, N. R. Newbury, W. M. Itano, D. J. Wineland, and J. C. Bergquist, "Frequency ratio of Al^+ and Hg^+ single-ion optical clocks; metrology at the 17th decimal place," *Science*, vol. 319, p. 1808, 2008.

[3] S. N. Lea, "Limits to time variation of fundamental constants from comparison of atomic frequency standards," *Rep. Prog. Phys.*, vol. 70, p. 1473, 2007.

[4] V. A. Dzuba, V. V. Flambaum, and M. V. Marchenko, "Relativistic effects in Sr, Dy, Yb II, and Yb III and search for variation of the fine-structure constant," *Phys. Rev. A*, vol. 68, p. 022506, 2003.

[5] V. A. Dzuba and V. V. Flambaum, "Relativistic corrections to transition frequencies of Ag I, Dy I, Ho I, Yb II, Yb III, Au I, and Hg II and search for variation of the fine-structure constant," *Phys. Rev. A*, vol. 77, p. 012515, 2008.

[6] C. Tamm, B. Lipphardt, H. Schnatz, R. Wynands, S. Weyers, T. Schneider, and E. Peik, "$^{171}\mathrm{Yb}^+$ single-ion optical frequency standard at 688 THz," *IEEE Trans. Instr. Meas.*, vol. 56, p. 601, 2007.

[7] K. Hosaka, S. A. Webster, A. Stannard, B. R. Walton, H. S. Margolis, and P. Gill, "Frequency measurement of the $^2\mathrm{S}_{1/2}-{}^2\mathrm{F}_{7/2}$ electric octupole transition in a single $^{171}\mathrm{Yb}^+$ ion," *Phys. Rev. A*, vol. 79, p. 033403, 2009.

[8] S. A. Webster, M. Oxborrow, and P. Gill, "Vibration insensitive optical cavity," *Phys. Rev. A*, vol. 75, p. 011801(R), 2007.

[9] B. R. Walton, H. S. Margolis, V. Tsatourian, and P.Gill, "A transportable optical frequency comb based on a mode-locked fibre laser," *IET Optoelectronics*, vol. 2, p. 182, 2008.

[10] G. P. Barwood, H. S. Margolis, G. Huang, P.Gill, and H. A. Klein, "Measurement of the electric quadrupole moment of the $4\mathrm{d}^2\mathrm{D}_{5/2}$ level in $^{88}\mathrm{Sr}^+$," *Phys. Rev. Lett.*, vol. 93, p. 133001, 2004.

[11] W. M. Itano, "External-field shifts of the $^{199}\mathrm{Hg}^+$ optical frequency standard," *J. Res. Natl. Inst. Stand. Technol.*, vol. 105, p. 829, 2001.

[12] T. Schneider, E. Peik, and C. Tamm, "Sub-hertz optical frequency comparisons between two trapped $^{171}\mathrm{Yb}^+$ ions," *Phys. Rev. Lett.*, vol. 94, p. 230801, 2005.

[13] D. J. Bate, K. Dholakia, R. C. Thompson, and D. C. Wilson, "Ion oscillation frequencies in a combined trap," *J. Mod. Opt.*, vol. 39, p. 305, 1992.

[14] I. Sherstov, B. Lipphardt, T. E. Mehlstäubler, M. Okhapkin, B. Stein, C. Tamm, and E. Peik, "Single-ion optical frequency standards with $^{171}\mathrm{Yb}^+$: Measurements of frequencies and frequency ratios," in *Proc. Eurpoean Frequency and Time Forum and IEEE International Frequency Control Symposium 2009*, 2009.

[15] H. R. Telle, B. Lipphardt, and J. Stenger, "Kerr-lens, mode-locked lasers as transfer oscillators for optical frequency measurements," *App. Phys. B*, vol. 74, p. 1, 2002.